doi: 10.1017/S143192760909343X
Microsc Microanal 15(Suppl 2), 2009


# Characterization of Continuous Cast AA2037 Al Alloy

E.A. Kenik*, Q. Zeng** and T. Zhai**
*Materials Science & Technology Division, Oak Ridge National Laboratory, Oak Ridge, TN, 37831
**Chemical & Materials Engineering Dept., University of Kentucky, Lexington, KY 40505

Continuous casting (CC) of aluminum alloys offers ~25% energy savings over its direct chill counterpart [1]. However, as a result of this simplified processing procedure (lack of ingot forming, homogenization and ingot breaking-down hot rolling), an inhomogeneous microstructure is expected, especially in the as-cast hot band. As part of the first time development to produce Al-Cu alloys via CC technology, the microstructure, mechanical properties and the impact of post-casting thermomechanical processing of AA2037 aluminum alloy need to be studied in order to optimize the properties of the alloy. It has been shown that homogenization near 475°C for 24 h prior to further processing results in a 28% increase in the fatigue limit compared to that for a shorter, higher temperature (510°C for 1 h) homogenization. Subsequent processing included water quenching, stretching by 3% and peak-aging at 150°C.

The AA2037 alloy (0.64Cu, 0.22Mn, 0.27Mg, 0.005Fe, 0.06Si, bal. Al (at.%)) was continuous cast using a twin belt caster. Mechanical properties and microstructure were characterized for the hot band as-cast and after various processing, including the two homogenization treatments mentioned above. Conventional TEM characterization (BF, DF and SA diffraction), Z-contrast STEM imaging, and EDS microanalysis were performed on conventionally electropolished disks. An FEI Tecnai20 ($LaB_6$) and a Philips CM200FEG were used for these respective tasks. X-ray microanalysis of fine precipitates is complicated by the relative size of the precipitate and the excited volume, which is determined by the incident probe size and beam broadening in the thin foil. By comparing the apparent composition indicated with the probe on the precipitate and in the adjacent matrix, the elements enriched in the precipitate can be identified.

Figure 1a and 1b show the microstructure of the material homogenized near 475ºC before and after a final 3% stretch/peak aging at 150ºC, respectively. The initial structure has coarse, equi-axed precipitates and dislocations presumably from the water quench. Dark-field imaging reveals that these dislocations are tangled around coarse precipitates. After peak aging, the equi-axed precipitates are still present, possibly with additional, smaller sized precipitates. At least one other phase is present as elongated precipitates (≤200 nm long). Quantitative comparisons of precipitate size and density are complicated by the inhomogeneous precipitate distribution reflecting the cast structure.

The utility of Z-contrast imaging in revealing the varied precipitate structure in these materials is obvious in Fig. 2(a,b). All precipitates containing higher atomic number elements can be visualized almost without regard for diffracting conditions. Based upon precipitate size and element enrichment, the precipitates could be divided into two major categories. The larger, roughly equi-axed precipitates are enriched in Mn with lower Fe, Si levels and traces of Cr, Ni. These latter four elements are not detected in the matrix. The maximum Mn level observed for the larger particles of this phase was ~10 at.%, which may give an estimate to the actual level present in this phase. The copper and Mg contents of this phase were difficult to determine, as the measured levels were similar to that of the adjacent matrix. The Mn-enriched precipitates ranged from ~2 μm down to ~30 nm in diameter (cf. Fig. 1,2). Prior to peak aging, only these Mn-enriched particles were present.

In the peak aged material a second category of precipitates was present, general smaller in size and enriched in copper, which appeared to sub-divide into at least two subgroups based on shape (roughly equi-axed versus elongated). The equi-axed Cu-enriched precipitates range from 100 nm down to 4 nm diameter. The elongated Cu-enriched precipitates range from ~300 nm down to 50 nm and were 4-10 nm thick when viewed edge-on. Most, but not all, Cu-enriched precipitates contain similar levels of copper and magnesium, including the elongated precipitates. From the elements enriched in this phase and electron diffraction, these precipitates are identified as the S′ phase. There were other shapes of Cu-enriched precipitates observed in Z-contrast images, including blocky and lens-shaped (e.g., Fig. 2c). It is possible that these other precipitates are other variants or truncated examples of the elongated, Cu-enriched S′ precipitates.[2]

1. X. F. Yu, X.Y. Wen, Y. M. Zhao and T. Zhai, Mater. Sci. Eng. A, **394** (2005) 376-384.
2. Research at the Oak Ridge National Laboratory SHaRE User Facility was sponsored by the Division of Scientific User Facilities, Office of Basic Energy Sciences, U.S. Department of Energy.

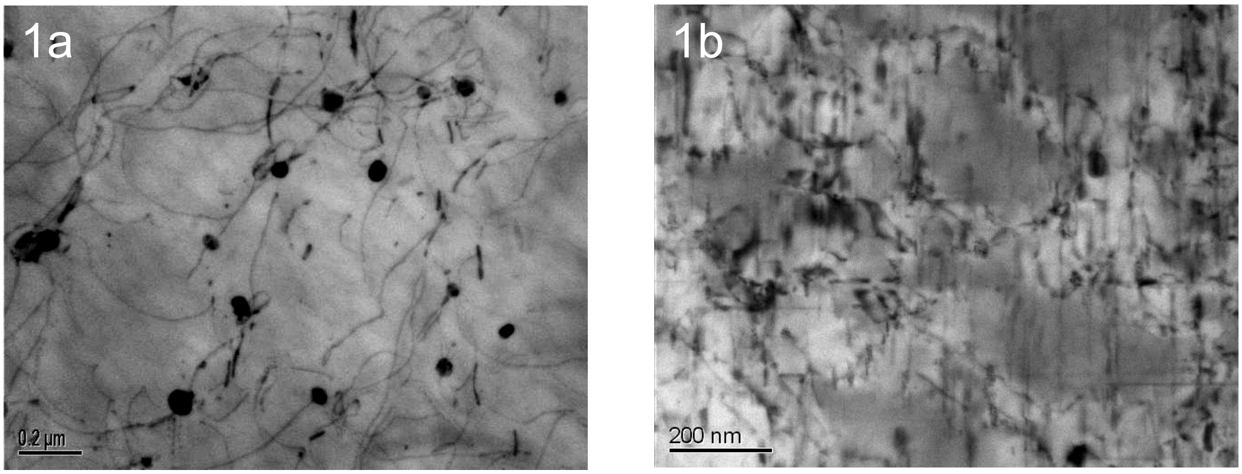


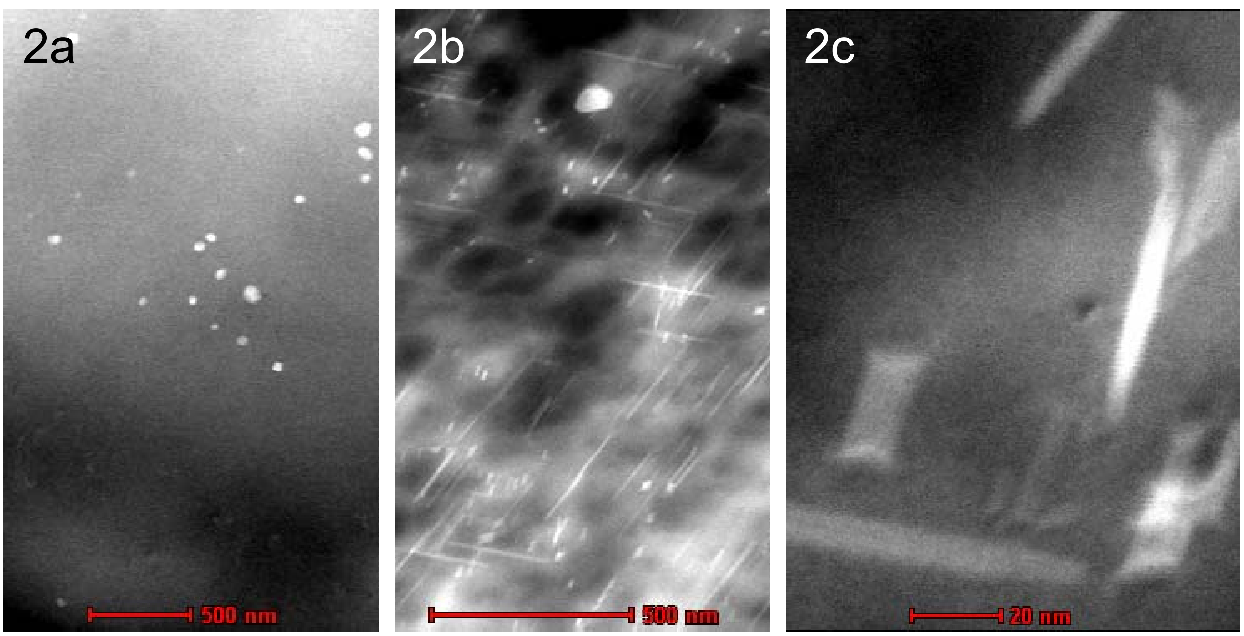


Fig. 1(a,b) – TEM of AA2037 alloy prior to (i.e., in the as-quenched condition) and after 3% stretching and aging to peak strength at 150°C, respectively. Note interaction of dislocations with precipitates in 1(a,b) and faint precipitates both vertically and horizontally in 1(b).
Fig. 2(a-c) – Z-contrast STEM images of AA2037 alloy (a) prior to and (b) after 3% stretching and aging to peak strength at 150°C. Blocky and lens-shaped Cu-enriched precipitates after peak aging.

https://doi.org/10.1017/S143192760909343X Published online by Cambridge University Press